Biochimica et Biophysica Acta, 985 (1989) 255–265
Elsevier

BBAMEM 74591

Correlation of enzyme activities with fluorescence anisotropy of dansyl-labeled cytochrome b_5/NADH–cytochrome-b_5 reductase systems in phosphatidylcholine vesicles

E.L. Pugh [1], M. Kates [1], A.G. Szabo [2] and D.T. Krajcarski [2]

[1] *Department of Biochemistry, University of Ottawa and* [2] *Division of Biological Sciences, National Research Council, Ottawa (Canada)*

(Received 22 March 1989)
(Revised manuscript received 5 July 1989)

Key words: Phosphatidylcholine vesicle; Fluorescence anisotropy; Cytochrome b_5; Cytochrome-b_5 reductase

The changes in steady-state fluorescence lifetimes and anisotropy decay parameters, as well as enzyme activities, of dansyl-labeled cytochrome b_5 (DNS-cytochrome b_5), on interaction with NADH–cytochrome-b_5 reductase in DMPC vesicles, have been measured as a function of temperature. Steady-state fluorescence of DNS-cytochrome b_5 in DMPC vesicles with and without cholesterol was increased on interaction with reductase at temperatures both above and below the DMPC phase transition. In all systems three fluorescence decay components of the dansyl label in DNS-cytochrome b_5 were observed. In the reductase-containing system, the long (major) decay time component of DNS-cytochrome b_5 and the fraction of the total fluorescence associated with this component increased over the temperature range 15–30°C. In time-resolved anisotropy measurements, the order parameters of DNS-cytochrome b_5 in DMPC vesicles increased on interaction with reductase at temperatures above the DMPC phase transition, and this increase was even more pronounced in cholesterol-containing vesicles, at temperatures from 15–30°C. The enzyme activity of the DNS-cytochrome-b_5 reductase system in DMPC vesicles was also greatly increased in the presence of cholesterol. These results show that interaction of vesicle-bound DNS-cytochrome b_5 and NADH–cytochrome-b_5 reductase leads to an increased degree of order of the dansyl-labeled cytochrome with little change in its rotational flexibility, and suggests that the increased order can be correlated with increased enzyme activity.

Introduction

The Δ^9- and Δ^5-desaturase systems of rat liver have been shown to contain three microsomal proteins [1–5]: NADH–cytochrome-b_5 reductase, cytochrome b_5 and terminal desaturase. The terminal Δ^9-desaturase has been reconstituted in lipid vesicles together with cytochrome b_5 and NADH–cytochrome-b_5 reductase [1].

Previous work from several laboratories has suggested that membrane-bound desaturase systems are regulated by the fluidity of the membrane phospholipids [1–8]. For example, an increased Δ^5-desaturase activity has been correlated with a decreased fluidity of rat liver microsomal membrane phospholipids [2–5]. Similar observations were made for the native [6] and reconstituted [1] Δ^9-desaturase of rat liver, the Δ^9-desaturase of *Tetrahymena* [7], and the Δ^{12}-desaturase of *Candida lipolytica* [2,3,8].

The interaction of the cytochrome-b_5 reductase and cytochrome b_5 has been shown to involve complementary charge pairs, including lysine residues on the reductase and carboxyl groups on the cytochrome b_5 [9,10]. The ion pair interactions between these two proteins, however, would be dependent, in part, on the physical properties of the lipid bilayer in which these proteins are anchored.

In order to elucidate the interactions and interrelationships of the three constituent proteins of the desaturase enzyme system, we have undertaken a study of two of these proteins, cytochrome b_5 and cytochrome-b_5 reductase, in lipid bilayers of defined order or fluidity. Our main approach in this paper has been to study the steady-state and time-resolved fluorescence properties and the fluorescence anisotropy parameters in recon-

Abbreviations: DNS-cytochrome b_5, dansyl-labeled cytochrome b_5; DMPC, dimyristoylphosphatidylcholine; Hepes, 4-(2-hydroxyethyl)-1-piperazineethanesulphonic acid; FAD, fluorescence anisotropy decay.

Correspondence: M. Kates, Department of Biochemistry, University of Ottawa, Ottawa, Ontario, Canada K1N 9B4.

stituted lipid/protein systems in the presence or absence of added cholesterol. However, because tryptophan fluorescence of cytochrome b_5 and cytochrome-b_5 reductase are indistinguishable, we have substituted the cytochrome b_5 with the dansyl (DNS) derivative [11], which can be studied under conditions where there is no tryptophan fluorescence.

This paper reports the changes in the fluorescence decay times and in the parameters obtained from time-resolved anisotropy measurements including rotational relaxation time and order parameters, as well as the enzyme activity, of vesicle-bound DNS-cytochrome b_5 on interaction with cytochrome-b_5 reductase, as a function of temperature. Our findings show that interaction of DNS-cytochrome b_5 and NADH–cytochrome-b_5 reductase had little effect on rotational flexibility of DNS-b_5 but led to an increased degree of order above the phase transition. In the presence of cholesterol, the degree of order of the system increased further and this was correlated with an enhanced enzyme activity.

Materials and Methods

Dimyristoylphosphatidylcholine (DMPC) and cholesterol were from Sigma, St. Louis, MO. Cholesterol was recrystallized twice from ethanol, and both lipids were found to be chromatographically pure on thin-layer chromatographic analysis by using silica gel H plates in the solvent system chloroform/methanol/water (65 : 35 : 5, v/v).

Preparation of cytochrome b_5 from bovine liver

Cytochrome b_5 from beef liver was prepared essentially by the procedure of Strittmatter et al. [12] modified to remove final traces of Triton X-100 (which is fluorescent), as follows. After purification of cytochrome b_5 on DEAE-cellulose and Sephadex as described [12], the protein, which still contained traces of Triton, was dialyzed against the buffer 5 mM Hepes, in 20 mM NaF, 20% glycerol, 0.05% Lubrol, 0.1 mM EDTA (pH 7.4) and loaded onto a Fractogel TSK DEAE-650(S) column. The column was washed with the buffer described above and cytochrome b_5 was then eluted with the second buffer containing 5 mM Hepes, 20 mM NaF, 20% glycerol, 70 mM $(NH_4)_2SO_4$, 0.05% Lubrol, 0.1 mM EDTA (pH 7.4). Fractions displaying an A_{413}/A_{280} of 2.2 were pooled and concentrated 10–20-fold on a PM-10 Amicon membrane. Residual traces of Lubrol were removed by passage through Sephadex G-25. The final preparation exhibited a single band on SDS-PAGE with a subunit M_r of 16600 and had a specific content of 45 nmol of cytochrome b_5 per mg of protein and an A_{413}/A_{280} ratio of 2.54, as reported previously for cytochrome b_5 [12–14]. The fluorescence emission spectrum of the highly purified cytochrome b_5 showed a single peak with an emission maximum of 338 nm (excitation at 280 or 290 nm), as reported previously for this cytochrome [15,16], and no fluorescence due to Triton X-100 at 300 nm.

Preparation of NADH–cytochrome-b_5 reductase from bovine liver

NADH–cytochrome-b_5 reductase from bovine liver was prepared by a modification of the procedure of Schafer and Hultquist [17] as follows. After purification of the reductase by ion-exchange and affinity chromatography, residual Triton X-100 and ADP were removed by chromatography on Fractogel TSK DEAE-650(S) as described above for cytochrome b_5. The final preparation had a specific activity of 1900 μmol of ferricyanide reduced per min per mg protein and exhibited an absorption spectrum with maxima at 273, 390 and 416 nm with a shoulder at 485 nm, in agreement with the values reported previously for this protein [17,18]. The purity of this preparation was determined by SDS-PAGE which showed only one band with a subunit M_r of 34500 (reported value: 34500 [17,18]). The fluorescence emission spectrum showed a single peak at 340 nm (excitation 280 or 290 nm) and no Triton fluorescence.

Preparation of DNS-cytochrome b_5

DNS-cytochrome b_5 was prepared and purified by the method of Gilmore and Glaser [11]. The amount of dansyl chloride incorporated into the protein was determined by difference absorption spectroscopy using an absorption coefficient of 3.36 $mM^{-1} \cdot cm^{-1}$ at 340 nm for the dansyl-protein conjugate [19]. DNS-cytochrome b_5 used in these studies was thus found to contain 1.0 ± 0.1 dansyl residues per mol cytochrome b_5.

Preparation of unilamellar lipid vesicles

Phospholipid vesicles were prepared by extrusion of DMPC in the absence and presence of 20 mol% cholesterol through polycarbonate filters according to the method of Hope et al. [20]. In these experiments, large multilamellar vesicles (1–2 mM) were prepared first by vortexing the appropriate amount of dry lipid in 100 mM Tris-acetate, 100 mM NaCl and 0.02% sodium azide. The resulting multilamellar vesicle dispersion was then extruded under pressure through standard polycarbonate filters (Nucleopore Corp., Pleasanton, CA) in a device produced by the National Research Council, Ottawa, Canada. The preparations used here were passed sequentially through filters having pore sizes of 0.4, 0.2 and 0.1 μm. All extrusion procedures were conducted above the phase transition temperature of the phospholipid (25 °C) and yielded unilamellar vesicles with average diameter 0.1 μm [20]. Similar fluorescence spectral results were obtained with vesicles prepared by sonication [11].

Preparation of protein-lipid complexes

DNS-cytochrome b_5 was incorporated into preformed phospholipid vesicles (prepared as described above) by a modification of the method of Gilmore and Glaser [11]. In these studies. 7.5 nmol of DNS-cytochrome b_5 in 10 mM Tris-acetate buffer (pH 8.1) was added to 750 nmol of lipid vesicles (prepared as in the above paragraph) in a final volume of 3 ml. The mixture was incubated at 30 °C for 8 h prior to the fluorescence measurements. In vesicles containing both DNS-cytochrome b_5 and NADH–cytochrome-b_5 reductase the amount of lipid was increased to 1.5 μmol and the reductase (7.5 nmol) was added after the addition of DNS-cytochrome b_5 (7.5 nmol). The mixture was then incubated at 30 °C as described above.

The binding of proteins to vesicles was confirmed by gel filtration on Sephadex G-200 as described elsewhere [21].

Assay procedures

Total lipids were extracted from vesicles by the modified method of Bligh and Dyer [22,23] and phospholipid was quantified by phosphate determination using a modified method of Bartlett [23,24]. For cholesterol analysis, total lipids were saponified by incubation for 1 h at 70 °C in 2M NaOH in methanol/water (5 : 1, v/v) according to the method of Rintoul et al. [25]. Unsaponifiable lipids (including cholesterol) were extracted with pentane and quantitated by gas-liquid chromatography on 3% SE-30 at 275 °C, with β-sitosterol as the internal standard as described earlier [4].

Cytochrome b_5 content was calculated from the absorbance at 413 nm using an absorption coefficient of 118 $mM^{-1} \cdot cm^{-1}$ [26] or from the reduced minus oxidized difference spectrum using an absorption difference of 185 $mM^{-1} \cdot cm^{-1}$ for $A_{424} - A_{409}$ [27]. NADH–cytochrome-b_5 reductase content was calculated from the absorbance at 461 nm, with an absorption coefficient of 11.3 $mM^{-1} \cdot cm^{-1}$ [28].

Cytochrome-*c* reductase activity was determined by the method of Jones and Wakil [29] using an absorption coefficient (550 nm) of 18.5 $mM^{-1} \cdot cm^{-1}$ [26], and NADH–ferricyanide reductase activity by the method of Spatz and Strittmatter [18] with an absorption coefficient (420 nm) of 1.02 $mM^{-1} \cdot cm^{-1}$ [18]. Protein was estimated by the method of Lowry et al. [30].

Fluorescence measurements

The fluorescence decay experiments were performed using the time-correlated single-photon counting technique with instrumentation described in detail elsewhere [31]. Essentially it included a Spectra Physics synchpumped argon ion dye laser and cavity dumper system as the excitation source, operating at 825 kHz and with a pulse width of 15 ps. The dye DCM was used in the dye laser to give an output at 680 nm. This in turn was frequency doubled to give the excitation wavelength of 340 nm which was vertically polarized. The emission was detected after passage through a polarizer set at 55° to the vertical and a JY H10 monochromator, with a 4 nm bandpass, on a Hamamatsu 1564U-01 microchannel plate photomultiplier. The channel width typically was 21.6 ps/channel and fluorescence decay curves were collected in 1024 channels of a multichannel analyzer (MCA). To optimize the signal-to-noise ratio, a minimum of 25 000 counts was usually collected in the peak of the sample profile. The ratio of laser pulses to single photon events was 100 : 1. A buffer blank was also measured under identical conditions as the corresponding sample.

For the fluorescence anisotropy decay experiments, the emission polarizer was set at 0° (vertical) to measure $I_\parallel(t)$, and at 90° (horizontal) to measure $I_\perp(t)$. Both these decay curves were measured for the same period of accumulation time. The instrument response function was determined by measuring the scattered light from a glycogen sample having an absorbance of 0.2 at the excitation wavelength. The buffer blank signal was subtracted from the sample decay curve giving appropriate consideration to the weighting of the data points [31]. The data were analyzed using the non-linear least-squares iterative convolution method based on the Marquardt algorithm. Adequacy of the exponential decay fitting was judged by the inspection of the plots of weighted residuals and other statistical parameters [32]. The standard error reported for the decay times in Fig. 4 indicates the precision of an individual decay experiment.

The '*G*' factor, or instrument sensitivity factor for the relative sensitivity of horizontally polarized and vertically polarized fluorescence in the time-correlated single-photon counting instrument was determined in the following way. The fluorescence decay curves, $I_\parallel(t)$ and $I_\perp(t)$, both measured for identical data collection times were integrated over all channels. These integral values were substituted into the expression for steady-state fluorescence anisotropy. The time-resolved instrument '*G*' factor was then calculated so that the fluorescence anisotropy value obtained from these integral values was equal to the steady-state anisotropy measurements.

Steady-state fluorescence measurements were made either on an SLM 8000C spectrofluorimeter equipped with a Neslab Endocal refrigerated circulating bath for temperature control, or a Perkin Elmer MPF 44A spectrofluorimeter. Absorption spectra were measured on a Cary 219 spectrophotometer. The excitation wavelength was 340 nm and the excitation and emission bandpass were both 4 nm. The absorbance of the samples was typically 0.1. Blank signals were subtracted from the spectra prior to plotting.

The steady-state fluorescence anisotropy was measured with vertically polarized excitation at 340 nm and an emission wavelength of 520 nm. 'T' format detection was used with a monochromator in each arm of the detection system. The emission bandpass was 8 nm. The polarizers used were 'so-called' ultraviolet calcite Glan-Thompson polarizers obtained through SLM-Aminco from Karl Lambrecht. The instrumental 'G' factor (I_{HV}/I_{HH}) was measured on each sample using horizontally polarized excitation. Each fluorescence intensity measurement was obtained after 10 s integration time, and the fluorescence anisotropy reported was the mean of at least three determinations. In every measurement the background signal was subtracted from the individual intensity values.

Results and Discussion

Fluorescence emission spectra of DNS-cytochrome b_5

Dansyl-labeled cytochrome b_5 prepared as described in Materials and Methods had a broad emission spectrum with an emission maximum of 525 nm (Fig. 1). The binding of DNS-cytochrome b_5 to DMPC vesicles resulted in an enhancement of fluorescence at tempera-

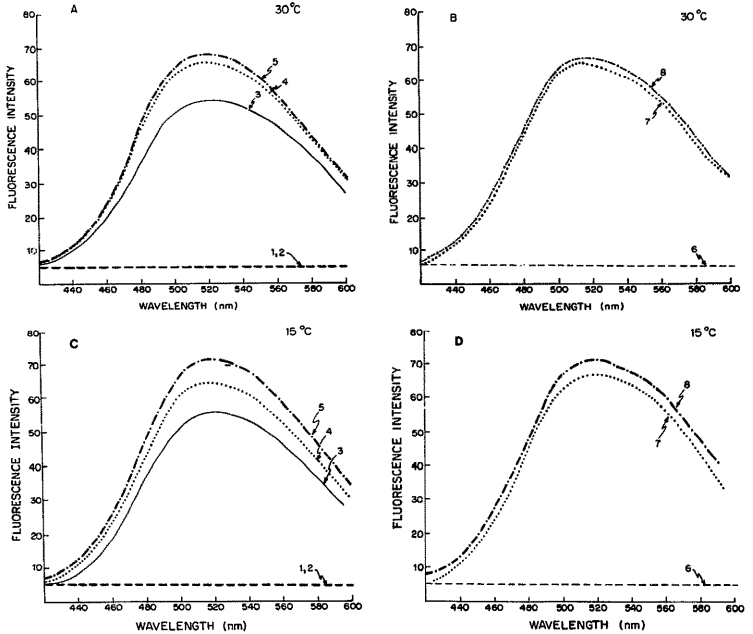

Fig. 1. Fluorescence emission spectra of DNS-cytochrome b_5 solutions in the absence and presence of NADH–cytochrome-b_5 reductase at (A) and (B) 30°C and (C) and (D) 15°C. 1, dimyristoylphosphatidylcholine vesicles; 2, NADH–cytochrome-b_5 reductase in dimyristoylphosphatidylcholine vesicles prepared by sonication; 3, DNS-cytochrome b_5 in buffer; 4, DNS-cytochrome b_5 in dimyristoylphosphatidylcholine vesicles; 5, DNS-cytochrome b_5 and NADH–cytochrome-b_5 reductase in dimyristoylphosphatidylcholine vesicles; 6, dimyristoylphosphatidylcholine vesicles containing 20 mol% cholesterol; 7, DNS-cytochrome b_5 in dimyristoylphosphatidylcholine vesicles containing 20 mol% cholesterol; 8, DNS-cytochrome b_5 and NADH–cytochrome-b_5 reductase in dimyristoylphosphatidylcholine vesicles containing 20 mol% cholesterol. The lipid/protein ratio was 100. Excitation was at 340 nm. Measurements were made on a Perkin Elmer 44A spectrofluorimeter.

tures both above and below the phase transition temperature of the phospholipid (curve 4, Fig. 1A and C). The fluorescence was enhanced further by the addition of an equimolar amount of NADH–cytochrome-b_5 reductase to the vesicles (curves 5, Fig. 1A and C), although the reductase itself did not fluoresce over the wavelengths measured (curve 2, Fig. 1A and C). The enhancement of the fluorescence of DNS-cytochrome b_5 by the inclusion of NADH–cytochrome-b_5 reductase in the vesicle was more pronounced at 15°C (8%) than at 30°C (3%).

The binding of DNS-cytochrome b_5 to DMPC vesicles containing 20 mol% cholesterol resulted in an enhancement of fluorescence intensity similar to that observed upon binding to vesicles containing DMPC alone both at 30 and 15°C (curve 7, Fig. 1B and D). The addition of NADH–cytochrome-b_5 reductase to the cholesterol-containing vesicles resulted in a further small enhancement of the fluorescence of DNS-cytochrome b_5 at both temperatures studied (curve 8, Fig. 1B and D).

Fluorescence decay times

The fluorescence decay times of DNS-cytochrome b_5 in solution and in DMPC and cholesterol-containing DMPC vesicles with and without reductase were determined as a function of temperature. A typical fluorescence decay curve of DNS-cytochrome b_5 is shown in Fig. 2. The fluorescence curves were analyzed in terms of sums of exponential decay components. The plots of weighted residuals (Fig. 3) for dansyl cytochrome b_5 in DMPC vesicles was typical for all analyses. The fits to single and double-exponential decay models are clearly inadequate (Fig. 3A and B). In each case the 'best fit' was one in which the decays were described by

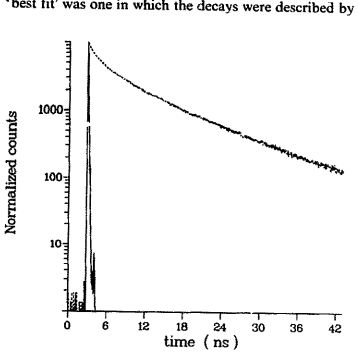

Fig. 2. Fluorescence decay of DNS-cytochrome b_5 as measured with a laser-based system; channel width, 22 ps; $\lambda_{ex} = 340$ nm; $\lambda_{em} = 520$ nm.

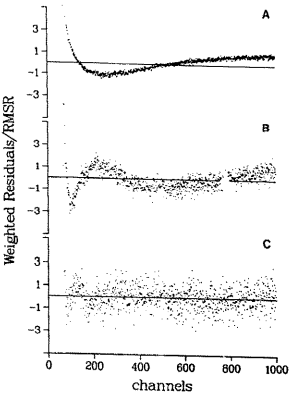

Fig. 3. Plots of weighted residuals for the 'best-fit' to the fluorescence decay data for DNS-cytochrome b_5 in DMPC vesicles at 24°C. (A) Single-exponential decay fit; (B) double-exponential decay fit; C, triple-exponential decay fit.

a sum of three exponential decay components (Fig. 3C). In each case the value of the longest decay time (τ_1) was found to range from 11.8 to 14.9 ns, depending on the sample (Fig. 4A). Similarly, the value of the intermediate decay component (τ_2) ranged from 3.4 to 4.7 ns (Fig. 4B). A third short component (τ_3) having a value close to 0.6 ns was found in all cases except for DNS-cytochrome b_5 in buffer where it had a value of 1.0 ns (data not shown).

The parameters at different temperatures and for the different mixtures for the two larger decay components are shown in Fig. 4. There was a small temperature dependency on the two longer decay times (τ_1 and τ_2) for each sample, changing by 6–10% over the temperature range studied (15–30°C). The effect of temperature on the value of the short decay time (τ_3) was negligible. The fractional fluorescence of the long decay component was 70–75%, the intermediate decay component was 22–27% and the short decay component was 3–4% of the total.

The values of τ_1 in DNS-cytochrome b_5 in DMPC or DMPC-cholesterol were similar to one another at each temperature (curves 2 and 3, Fig. 4A). The addition of reductase to either sample resulted in a significant increase in the value of τ_1. Again τ_1 values (Fig. 4A, curves 4 and 5) in these latter cases were nearly identical at each temperature, except that in the case of the DNS-cytochrome b_5/ DMPC–cholesterol/ reductase

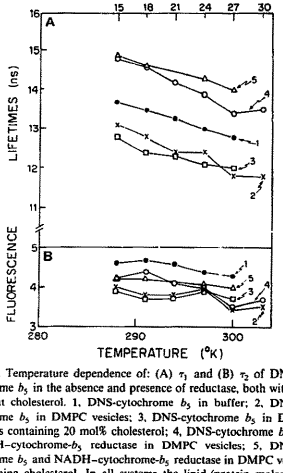

Fig. 4. Temperature dependence of: (A) τ_1 and (B) τ_2 of DNS-cytochrome b_5 in the absence and presence of reductase, both with and without cholesterol. 1, DNS-cytochrome b_5 in buffer; 2, DNS-cytochrome b_5 in DMPC vesicles; 3, DNS-cytochrome b_5 in DMPC vesicles containing 20 mol% cholesterol; 4, DNS-cytochrome b_5 and NADH–cytochrome-b_5 reductase in DMPC vesicles; 5, DNS-cytochrome b_5 and NADH–cytochrome-b_5 reductase in DMPC vesicles containing cholesterol. In all systems the lipid/protein molar ratio was 100. Values are the mean of two measurements with a standard error in each of ±0.01 ns.

system (curve 5 Fig. 4A), τ_1 was greater above 20°C compared to the system lacking cholesterol (curve 4, Fig. 4A). The same trends were observed in τ_2 (Fig. 4B).

The increase in τ_1, in the presence of reductase was accompanied by an increase in the fraction of the total fluorescence (F_1) associated with this lifetime component. F_1 was 0.70 in DMPC and cholesterol-containing DMPC vesicles, but increased to 0.75 on the addition of reductase to these vesicles (data not shown). On the other hand, the fraction of the total fluorescence associated with τ_2, (F_2) decreased from 0.26 and 0.27 in DMPC and cholesterol-containing DMPC vesicles, respectively, to 0.22 on the addition of reductase. The fractional fluorescence associated with τ_3 was the same (3–4%) in all systems.

The increase in τ_1 and F_1 on addition of reductase parallels the observed increase in steady-state fluorescence (Fig. 1). The higher values of τ_1, which result in increases in F_1 may be due to an association of DNS-cytochrome b_5 with reductase which reduces the efficiency of collisional deactivation of the DNS-labeled cytochrome. The lack of any change in fractional fluorescence suggests that there is not a large change in the conformational distribution of the DNS-labeled segment of cytochrome b_5.

It should be noted that fluorescence lifetimes of DNS-cytochrome b_5 have been reported earlier [11] in systems lacking reductase and/or cholesterol. In the absence of reductase and cholesterol, our fluorescence lifetime measurements differ significantly from the reported values [11]. The earlier measurements were made with a single frequency phase and modulation fluorimeter. Since that time considerable progress has been made in the resolution capabilities of fluorescence decay instrumentation [31]. In the present studies, a time-correlated single-photon counting fluorescence lifetime instrument using pulsed laser excitation was used. The values reported earlier by Gilmore and Glaser [11] correspond to the mean value of those reported in this paper.

Steady-state anisotropy

The steady-state anisotropy of DNS-cytochrome b_5 in DMPC and cholesterol-containing DMPC vesicles with and without reductase was determined as a function of temperature. In all systems the steady-state anisotropy decreased slightly (5–10%) with increasing temperature (Fig. 5). Anisotropy values did not change much from one system to another, and only slight differences were observed on addition of reductase and/or cholesterol.

Fluorescence anisotropy decay

The fluorescence anisotropy decay (FAD) of DNS-cytochrome b_5 in DMPC and cholesterol/DMPC

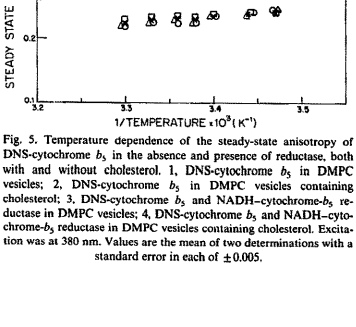

Fig. 5. Temperature dependence of the steady-state anisotropy of DNS-cytochrome b_5 in the absence and presence of reductase, both with and without cholesterol. 1, DNS-cytochrome b_5 in DMPC vesicles; 2, DNS-cytochrome b_5 in DMPC vesicles containing cholesterol; 3, DNS-cytochrome b_5 and NADH–cytochrome-b_5 reductase in DMPC vesicles; 4, DNS-cytochrome b_5 and NADH–cytochrome-b_5 reductase in DMPC vesicles containing cholesterol. Excitation was at 380 nm. Values are the mean of two determinations with a standard error in each of ±0.005.

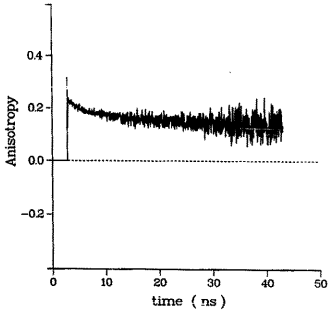

Fig. 6. Decay of fluorescence anisotropy for DNS-cytochrome b_5 in DMPC vesicles calculated according to Eqn. 1 at 21°C.

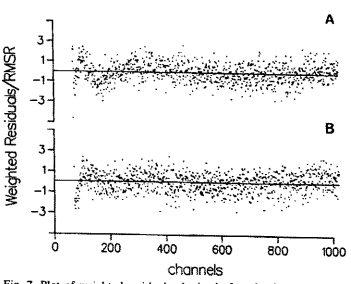

Fig. 7. Plot of weighted residuals obtained after simultaneous fitting of (A) $I_{\parallel}(t)$; and (B) $I_{\perp}(t)$ according to Eqns. 2, 3 and 4 where the data were fitted to a single rotational relaxation time, β, and a single r_{∞} value.

vesicles with and without added reductase was determined as a function of temperature. A typical FAD curve of DNS-cytochrome b_5 in DMPC is shown in Fig. 6. This curve was determined according to the equation

$$R(t) = I_{\parallel}(t) - I_{\perp}(t) \cdot G / I_{\parallel}(t) + 2I_{\perp}(t) \cdot G \quad (1)$$

where $R(t)$ is rate of decay; $I_{\parallel}$ and $I_{\perp}$ are the parallel and perpendicular fluorescence intensities, respectively; and G represents the correction factor for the instrumental sensitivity in each polarization direction. It is clear that the fluorescence anisotropy decays in a moderate time (< 10 ns) to a significant plateau value. These curves required analysis using exponential decay terms as well as a constant r_{∞} value. The decay curves, $I_{\parallel}(t)$ and $I_{\perp}(t) \cdot G$ were analysed simultaneously using the global method [33] according to the equations:

$$I_{\parallel}(t) = 1/3 \Sigma \alpha_i \exp - t/\tau_i (1 + 2r(t)) \quad (2)$$

$$I_{\perp}(t) = 1/3 \Sigma \alpha_i \exp - t/\tau_i (1 - r(t)) \quad (3)$$

$$r(t) = (r_0 - r_{\infty}) \exp - t/\beta + r_{\infty} \quad (4)$$

In every case satisfactory fits to the fluorescence anisotropy decay data were obtained when it was analysed in terms of a single relaxation time, β, which characterizes the motion of the dansyl group, and a fluorescence anisotropy plateau value equivalent to r_{∞} and an initial fluorescence anisotropy value of r_0, as written above (Fig. 7.) In Eqns. 2 and 3, the part $\Sigma \alpha_i \exp - t/\tau_i$ represents the fluorescence decay expression of the DNS-cytochrome b_5. In the fitting procedure for the two anisotropy decay curves this part of the expression was also allowed to vary and the best-fit values found. In every case the fluorescence decay times, τ_i, agreed very well with those found from a 'magic angle' experiment where only the fluorescence decay behaviour was determined. The results for β, the rotational relaxation time are shown in Fig. 8. At 15°C, the values ranged from 9.6 ns for the DNS-cytochrome b_5/reductase sample (Fig. 8) to 8.0 ns for the DNS-cytochrome b_5/cholesterol sample). As the temperature increased, the values of β decreased significantly and progressively for all samples. The experimental error in the determination of β was ±0.3–0.5 ns. For the DNS-cytochrome b_5, DNS-cytochrome b_5/reductase and DNS-cytochrome b_5/reductase + cholesterol samples there appears to be a discontinuity near 24°C, this discontinuity being more pronounced in the latter sample. The value of β at all

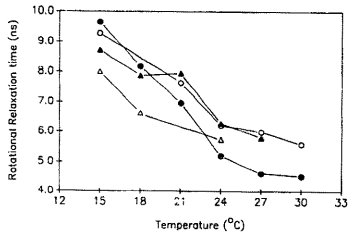

Fig. 8. Temperature dependence of the rotational relaxation times of DNS-cytochrome b_5 in the absence and presence of reductase, both with and without cholesterol. ○, DNS-cytochrome b_5 in DMPC vesicles; △, DNS-cytochrome b_5 in DMPC vesicles containing cholesterol; ●, DNS-cytochrome b_5 and reductase in DMPC vesicles; ▲, DNS-cytochrome b_5 and reductase in DMPC vesicles containing cholesterol. Values are the means of two measurements with a standard error in each of ±0.3-0.5 ns.

temperatures above 15°C was lower when reductase was added to DNS-cytochrome b_5 (Fig. 8). This suggests that the dansyl probe segment of the labelled cytochrome b_5 experiences increased flexibility or motion when the enzyme was added. Above 24°C, the addition of cholesterol to this latter sample resulted in the dansyl segment retaining the same flexibility as in the DNS-cytochrome b_5 sample (Fig. 8).

Rotational relaxation times of DNS-cytochrome b_5 in DMPC vesicles have been determined previously [11], in systems lacking the reductase. The values of relaxation times reported in the present paper in the absence of reductase differ from those reported earlier. In the previous study the steady-state anisotropy was used to calculate β and no estimate of r_∞ was made. The relaxation times were calculated from the Perrin relationship, while in the present work they were directly measured. The plateau behaviour of the fluorescence anisotropy decay reported in this work shows that the dansyl motion is anisotropic and does not decay to a zero value as is assumed in the Perrin formula. This can easily explain the different values reported herein.

Order parameters

In every case the fluorescence anisotropy decayed to a plateau value, r_∞, which was greater than zero (Fig. 6). This indicates that the dansyl probe label was not located in an isotropic environment and experiences restricted motion. In studies using lipid polyene probes [34,35] in membranes, when this behaviour was observed an order parameter, S, could be estimated from the expression:

$$S = (r_\infty / r_0)^{1/2} \tag{5}$$

where r_∞ is the plateau value of the fluorescence anisotropy at long time, and r_0 is the initial fluorescence anisotropy at time zero. The order parameter is a term which describes the equilibrium orientational distribution of the probe. It has sometimes been used to estimate the semi-angle of a cone in which the probe can freely diffuse [36]. When the anisotropy of a probe molecule such as dansyl clearly decays to a plateau and does not very slowly further decay to zero, then an order parameter, S, of the probe can be simply calculated from the above equation (Eqn. 5). Table I gives some representative values of r_0, r_∞ and S at 18°C for the complexes investigated.

The data show that the order of the dansyl label on the cytochrome b_5 is very high. This suggests, as well, that there is a very limited range of motion of the probe. The order parameters at all other temperatures are presented in Fig. 9. The values range from 0.77 to 0.89 depending on the system.

Several points are noteworthy. The most important is that both the order parameter, S, and the rotational

TABLE I

Values of r_0, r_∞, and S at 18°C for DNS-cytochrome b_5 systems measured

Components in DMPC	r_0	r_∞	S
DNS-cyt b_5	0.231	0.157	0.825
DNS-cyt b_5/Chol *	0.306	0.229	0.865
DNS-cyt b_5/Red *	0.230	0.156	0.825
DNS-cyt b_5/Red/Chol *	0.337	0.263	0.885

* Abbreviations: Chol, cholesterol; Red, cyt b_5 reductase.

relaxation time, β, decrease with increasing temperature, but that the steady-state anisotropy, $\langle r \rangle$, (Fig. 5) hardly changes with temperature or from sample to sample. At first consideration this was unexpected, and if one calculates a value of $\langle r \rangle$ from the Perrin relationship [37]:

$$\frac{r_0}{\langle r \rangle} = \frac{r_0 - r_\infty}{\left(1 + \frac{\tau}{\beta}\right)} + r_\infty$$

a value of $\langle r \rangle$ for DNS-cytochrome b_5 DMPC of 0.19 and for DNS-cytochrome b_5-DMPC/cholesterol, 0.26, which do not coincide with the measured steady-state values if only the long decay time component is used in the calculation. However, in treating the anisotropy decay data, the integrated average anisotropy values were made equal to the steady-state values through the 'G' factor instrument correction (see Material and Methods). The reason for this discrepancy may be because the average decay time is significantly less than the long decay time value and this would alter the calculated value of $\langle r \rangle$. In addition, the β value obtained may be a weighted average of the correlation times of each decay time component, i.e., each decay component may have a different value of β_A [38]. At the present time we are unable to resolve the correlation time into its individual components.

On comparison of DNS-cytochrome b_5 in the presence and absence of reductase (Fig. 9) below the phase transition of DMPC (24°C), at 21 and 18°C, the order parameters were found to be identical. We cannot account for the difference in values at 15°C. Above 24°C, the order parameter is higher for the DNS-cytochrome b_5/reductase sample. This must reflect an interaction between the two proteins and an increased degree of order on the cytochrome b_5 when reductase is present. Reductase then reduces the range of motion of the probe. A second point which is most significant is that cholesterol has a substantial effect on the order parameter. For example, at 27°C the order parameter for DNS-cytochrome b_5 in DMPC was 0.78, while on addition of cholesterol the order parameter increased to a value of 0.85. In every case, except the DNS-cytochrome b_5/cholesterol/reductase system, the order

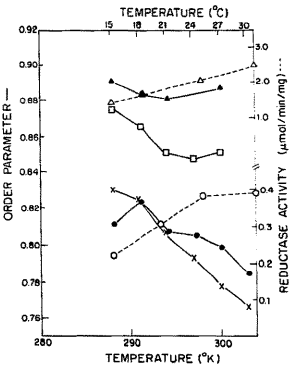

Fig. 9. Order parameters of DNS-cytochrome b_5 in the absence and presence of reductase both with and without cholesterol as a function of temperature. ×, DNS-cytochrome b_5 in DMPC vesicles; □, DNS-cytochrome b_5 in DMPC vesicles containing cholesterol; ●, DNS-cytochrome b_5 and reductase in DMPC vesicles; ▲, DNS-cytochrome b_5 and reductase in DMPC vesicles containing cholesterol. The dotted lines represent the cytochrome-*c* reductase activity of: ○, DNS-cytochrome b_5 and reductase in DMPC vesicles; and ▵, DNS-cytochrome b_5 and reductase in DMPC vesicles containing cholesterol.

parameter decreases with temperature. In this exceptional case there is hardly any temperature variation of the order parameter. On the addition of cholesterol or reductase to DNS-cytochrome b_5, the change with temperature was less than that observed for DNS-cytochrome b_5 alone. In the case of DNS-cytochrome b_5/cholesterol an apparent plateau value of the order parameter was obtained.

Comparison of the curves in Fig. 9, which correspond to the sample of DNS-cytochrome b_5/reductase in the presence and absence of cholesterol, respectively, shows that again cholesterol has a dramatic effect on the order parameter. The enzyme activities of DNS-cytochrome b_5/reductase in the presence and absence of cholesterol (Fig. 9) show that there is a direct correlation between the enzyme activity and the order parameter. These data show that cholesterol markedly increases the order parameter associated with cytochrome b_5 and this is accompanied by a significant increase in the enzyme activity at all temperatures in the presence of cholesterol (Fig. 9).

It is recalled that above the phase transition of DMPC, the relaxation time, β, of all samples are nearly the same, except for those values obtained for the DNS-cytochrome b_5/reductase system (Fig. 8). In this latter case the relaxation time was approx. 4.5 ns, a value almost 1.5 ns less than observed for the other systems. This shows that the rate of motion of the cytochrome b_5 in this system is more rapid. The increased order of this same system indicates that the cytochrome b_5 must have assumed a more ordered conformation on interaction with the reductase enzyme.

Enzyme activities

When DMPC vesicles containing DNS-cytochrome b_5 and NADH–cytochrome-b_5 reductase were assayed for reductase activity with cytochrome *c* as the electron acceptor in the temperature range 10–30 °C, the resulting Arrhenius plot showed a linear increase with temperature and a discontinuity at 25 °C, near the phase

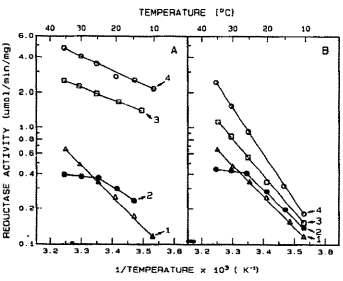

Fig. 10. Temperature dependence of the cytochrome-*c* reductase activity of: (A) DNS-cytochrome b_5 and NADH–cytochrome-b_5 reductase; and (B) native cytochrome b_5 and NADH–cytochrome-b_5 reductase in: 1, buffer; 2, DMPC vesicles; and 3, DMPC vesicles containing 20 mol% cholesterol: curve 4, temperature dependence of the ferricyanide reductase activity of samples 1–3. Cytochrome *c* and ferricyanide reductase activities were determined as described in Materials and Methods. Activities are the average of three determinations with a deviation of ±5%.

TABLE II

Aparent activation energies

Sample	Activation energy (E_a) kJ/mol
Cytochrome *c* reductase activity	
Cyt b_5/reductase/buffer (curve 1, Fig. 10B)	49
Cyt b_5/reductase/DMPC (curve 2, Fig. 10B)	
below T_m	51
above T_m	8
Cyt b_5/reductase/DMPC/Chol (curve 3, Fig. 10B)	58
DNS-b_5/reductase/buffer (curve 1, Fig. 10A)	49
DNS-b_5/reductase/DMPC (curve 2, Fig. 10A)	
below T_m	26
above T_m	3
DNS-b_5/reductase/DMPC/Chol (curve 3, Fig. 10A)	26
Ferricyanide reductase activity	
Cyt b_5/reductase/buffer DMPC or DMPC-Chol (curve 4, Fig. 10B)	76
DNS-b_5/reductase/buffer, DMPC or DMPC-Chol (curve 4, Fig. 10A)	23

transition (23–24°C) of the phospholipid vesicles (Fig. 10A, curve 2). The presence of cholesterol in the bilayer abolished the discontinuity in the Arrhenius plot and resulted in a greater than 5-fold increase in activity of the labeled protein at all temperatures measured (Fig. 10A, curve 3).

Similar results were found for the native cytochrome b_5/cytochrome-b_5 reductase/cytochrome *c* system in the absence of cholesterol (Fig. 10B, curve 2), but in the presence of cholesterol the increase in activity was only 1.4–2.8-fold (Fig. 10B, curve 3). We have no explanation for this observation, but it should be pointed out that the dansyl group is located in the membrane-binding fragment of cytochrome b_5 [11] which may result in a stronger binding to the DMPC-cholesterol vesicle and interaction of the active site with cytochrome *c*.

Note that the linear plot of cytochrome-*c* reductase activity of the native cytochrome b_5/cytochrome-b_5 reductase system in buffer (Fig. 10B, curve 1) was identical to that of the DNS-cytochrome b_5 system in buffer (Fig. 10A, curve 1). Also, the linear plot of activities obtained with ferricyanide as electron acceptor gave a higher activation energy (Table II) and higher activities than in the presence of cytochrome *c* for the native cytochrome b_5 systems (Fig. 10B, curve 4). Ferricyanide reductase activities for the DNS-cytochrome b_5 systems (Fig. 10A, curve 4) were even higher at all temperatures than the cytochrome *c* activities (Fig. 10A, curves 1, 2 and 3) and the activation energies were lower than that for the cytochrome *c* activity in buffer (Table II).

No significant differences in activation energy were observed between the native cytochrome b_5 systems in buffer, in DMPC vesicles alone below T_m or in DMPC vesicles with cholesterol (Table II). However, above T_m the vesicle-bound system without cholesterol has a greatly reduced activation energy (Table II) and a lower activity (Fig. 10B, curve 2) than in vesicles containing cholesterol. Similar observations were made in the DNS-cytochrome b_5-containing systems (see Fig. 10A, Table II).

Conclusion

Our observations on the change in the anisotropy decay parameters and the fluorescence lifetimes of vesicle-bound DNS-cytochrome b_5 on interaction with NADH–cytochrome-b_5 reductase suggest a specific interaction of the two proteins which leads to an increased ordering of the DNS-cytochrome b_5 but little change in its rotational flexibility. This conclusion is supported by: (1) the increase in the long-lifetime component (τ_1) of DNS-cytochrome b_5 on interaction with reductase, which suggests a special association of the two proteins; (2) the increase in the order parameter which indicates an increased degree of order in the reductase-containing system; and (3) the same changes in rotational relaxation time which indicate similar rotational flexibility. It should be noted that an even stronger interaction of cytochrome b_5 with cytochrome-b_5 reductase occurs in vesicles containing 20% cholesterol, similar to the cholesterol content of microsomal membranes [4]. The increased degree of order of DNS-cytochrome b_5 on interaction with reductase would suggest changes in the secondary structure of DNS-cytochrome b_5.

In this regard, recent FT-IR [39] studies have indicated that changes in protein secondary structure occur on interaction of cytochrome b_5 with cytochrome *c*. In the FT-IR studies [39], the changes could not be assigned to cytochrome b_5, but our studies suggest that changes in the secondary structure of this cytochrome may occur on interaction with other proteins (e.g., the cytochrome b_5 reductase).

Acknowledgements

This study was supported by grants from the Ontario Heart and Stroke Foundation and the Natural Sciences and Engineering Research Council of Canada. The technical assistance of Mr. Ian Fachnie is acknowledged.

References

1 Enoch, H.G., Catala, A. and Strittmatter, P. (1976) J. Biol. Chem. 251, 5095–5103.

2 Kates, M. and Pugh, E.L. (1980) in Membrane Fluidity: Biophysical Techniques and Cellular Regulation (Kates, M. and Kuksis, A., eds.) pp. 153–170, Humana Press, Inc., Clifton, NJ.
3 Kates, M., Pugh, E.L. and Ferrante, G. (1984) in Biomembranes, Vol. 12, (Kates, M. and Manson, L.A., eds.), pp. 379–395, Plenum Press, New York.
4 Pugh, E.L., Kates, M. and Szabo, A.G. (1980) Can. J. Biochem. 58, 952–958.
5 Pugh, E.L., Kates, M. and Szabo, A.G. (1982) Chem. Phys. Lipids 30, 55–69.
6 Lippiello, P.M., Holloway, C.T., Garfield, S.A. and Holloway, P.W. (1979) J. Biol. Chem. 254, 2004–2009.
7 Martin, C.E. and Thompson, G.A. (1978) Biochemistry 17, 3581–3586.
8 Ferrante, G. and Kates, M. (1983) Can. J. Biochem. Cell Biol. 61, 171–177.
9 Dailey, H.A. and Strittmatter, P. (1979) J. Biol. Chem. 254, 5388–5396.
10 Dailey, H.A. and Strittmatter, P. (1980) J. Biol. Chem. 225, 5184–5189.
11 Gilmore, R. and Glaser, M. (1982) Biochemistry 21, 1673–1680.
12 Strittmatter, P., Fleming, P., Connors, M. and Corcoran, D. (1978) Methods Enzymol. 51, 97–101.
13 Ozols, J. (1974) Biochemistry 13, 426–434.
14 Tamburini, P.P., White, R.E. and Schenkman, J.B. (1985) J. Biol. Chem. 260, 4007–4015.
15 Dufourcq, J., Faucon, J.F., Lussan, C. and Bernon, R. (1975) FEBS Lett. 57, 112–116.
16 Leto, T.L. and Holloway, P.W. (1979) J. Biol. Chem. 254, 5015–5019.
17 Schafer, D.A. and Hultquist, D.E. (1980) Biochem. Biophys. Res Commun. 95, 381–387.
18 Spatz, L. and Strittmatter, P. (1973) J. Biol. Chem. 248, 793–799.
19 Hartley, B.S. and Massey, V. (1956) Biochim. Biophys. Acta 21, 58–65.
20 Hope, M.J., Bally, M.B., Webb, G. and Cullis, P.R. (1985) Biochim. Biophys. Acta 812, 55–65.
21 Freire, E., Markello, T., Rigell, C. and Holloway, P.W. (1983) Biochemistry 22, 1675–1680.
22 Bligh, E.G. and Dyer, W.J. (1959) Can. J. Biochem. Physiol. (1959) 37, 911–917.
23 Kates, M. (1986) Techniques of Lipidology, Elsevier, Amsterdam.
24 Bartlett, G.R. (1959) J. Biol. Chem. 234, 466–468.
25 Rintoul, D.A., Chou, S.-M. and Silbert, D.F. (1979) J. Biol. Chem. 254, 10070–10077.
26 Rogers, M.J. and Strittmatter, P. (1973) J. Biol. Chem. 248, 800–806.
27 Omura, T. and Sato, R. (1964) J. Biol. Chem. 239, 2370–2378.
28 Mihara, K., Sato, R., Sakakibara, R. and Wada, H. (1978) Biochemistry 17, 2829–2834.
29 Jones, P.D. and Wakil, S. J. (1967) J. Biol. Chem. 242, 5267–5273.
30 Lowry, O.H., Rosebrough, N.J., Farr, A.L. and Randall, R.J. (1951) J. Biol. Chem. 193, 265–275.
31 Zuker, M., Szabo, A.G., Bramall, L. and Krajcarski, D.T. (1985) Rev. Sci. Instrum. 56, 14–22.
32 McKinnon, A.E., Szabo, A.G. and Miller, D.R. (1977) J. Phys. Chem. 81, 1564–1570.
33 Cross, A.J. and Fleming, G.R. (1984) Biophys. J. 46, 45–56.
34 Heyn, M.P. (1979) FEBS Lett. 108, 359–364.
35 Zannoni, C., Arcioni, A. and Cavatorta, P. (1983) Chem. Phys. Lipids 32, 179–250.
36 Lipari, G. and Szabo, A. (1980) Biophys. J. 30, 489–506.
37 Hildenbrand, K. and Nicolau, C. (1979) Biochem. Biophys. Acta 553, 365–377.
38 Ludescher, R.D., Peting, L., Hudson, S. and Hudson, B. (1987) Biophys. Chem. 28, 59–75.
39 Holloway, P.W. and Mantsch, H.H. (1988) Biochemistry 27, 7991–7993.